Improvement of Photogrammetric Quality of the 3-Fold Stereoscopic Linescan Camera MEOSS by Gauss-Markov Models of Satellite Dynamics

DRESCHER,A., MASAHARU,H.[1]) GILL,R., LEHNER,M.

DFVLR, German Aerospace Establishment, Inst. of Optoelectronics, D-8031 Oberpfaffenhofen

Abstract

The MEOSS camera of DFVLR generates three differently inclined scan planes by 3 parallel CCD linear arrays in one common focal plane. In the case of flat terrain this imaging geometry shows low inherent stability for photogrammetric block adjustment. Therefore correlations of neighbouring observation stations by Gauß-Markov processes are introduced as pseudo observation equations. Characteristics of satellite orbit and attitude dynamics are analysed to define order and weight of the process. Suitability of this approach was studied by simulation.

1. Introduction

Threefold stereoscopic linescan cameras were planned for STEREOSAT and MAPSAT missions. Stereo-MOMS, a high resolution camera of similar type is now under development for the German D-2 space-lab mission. An earlier and more prolonged test and demonstration of the capabilities of this camera type is expected from MEOSS, a German-Indian satellite mission. Launch of the medium resolution MEOSS camera is expected in mid 1988. Detailed information on technical, mission and application aspects of MEOSS is given in this supplements by F.Lanzl (1).

Definition of geometric relations between the three continuous image stripes can be tried in different ways. The main concepts are based either on orbit and attitude control, as planned for MAPSAT, or on photogrammetric analysis as planned for MEOSS and Stereo-MOMS. The image-coordinates of homologous points HP's representing the same ground feature in all three image stripes are used to feed the photogrammetric analysis.

Since the orientation parameters OP's (position and attitude) are continuously changing in case of linescanners, only a line-triplet LT, a momentary image of MEOSS, can be of metric quality. For MEOSS the OP's of the LT's will be estimated at regular time intervals (orientation intervals OI's) with linear interpolation in between. This scheme was originally proposed by Ebner (2).

---

[1]) Geographical Survey Institute, Tsukuba-Shi,305 Japan, staying at DFVLR from July '87 to March '89 as a visiting scientist.

The OP's of the MEOSS camera will be correlated by HP's with a stepwidth of one baselength B. In case of constant height and flight velocity over flat terrain the analysis by HP's is becomming unstable as shown first by Hofmann (3). The reason is, that indiviual correlation chains of stepwidth B, which start at different positions (phase) within the first B stay independent. Drescher et al. (4) indicated that certain periodic changes of orientation parameters OP's, which are resonant to the baselength B, can be equivalently interpreted by constant OP's and periodic terrain profiles (resonance problem).

To avoid this mathematical ambiguity, additional models, constants or pseudo observations have to be introduced.

2. The Simulation Software SAEROS

To allow sytematic studies of the effects of satellite dynamics and different densities of OI's, HP's and ground control points GCP's, DFVLR built up the simulation software SAEROS in a joint effort with University of Hannover. The main work was done and published by J.Wu (5).

Observation equations of least square fitting in the SAEROS simulation software are given as follows. Symbols are mostly in accordance with Manual of Photogrammetry, 4th edition, chapter 2.6.

1. linearizied collinearity equation for one imaging ray (homologous point j is imaged between orientation stations i and i + 1):

$$v_{ij} + \dot{B}_{ij} \begin{pmatrix} \dot{\Delta}_i \\ \dot{\Delta}_{i+1} \end{pmatrix} + \ddot{B}_{ij} \ddot{\Delta}_j = \epsilon_{ij}$$

(2,1) (2,12) (12,1) (2,3)(3,1) (2,1)

$\dot{\Delta}_i$: corrections to exterior orientation parameters
$\ddot{\Delta}_j$: corrections to ground point coordinates

2. ground control equations for point j:

$$\ddot{v}_j - I \ \ddot{\Delta}_j = X_j^0 - X_j^{00}$$

(3,1) (3,3)(3,1) (3,1) (3,1)
X_j^0 : approximation of ground coordinates used for linearized equation.
X_j^{00} : known or observed ground coordinates of control point j

3. Gauß process model of second order, Markov constant β set to unity (orientation stations i, i+1, i+2 are then related by this equation):

$$\dot{v}_i = (P_i - P_{Ni}) - 2(P_{i+1} - P_{N,i+1}) + (P_{i+2} - P_{N,i+2})$$

P_i : external orientation parameters of station i
P_{Ni} : nominal value of external orientation parameters of station i. Initial approximations are used as nominal values.

The system of the reduced normal equations is solved by recursive partitioning and Cholesky factorization.

3. Simulation with SAEROS

3.1 Constant Input Parameters

Up to now all simulations were made in a rectangular coordinate system, excluding the effects of earth curvature and earth rotation. On the other hand time variations of the input orientation parameters were always idendical to (5) in accordance with expected satellite dynamics. Details on orbit and attidude dynamics of the Indian SROSS satellite are given in (4) and actualized in (1).

The input profile of the orientation parameters used in all simulation runs is shown in fig. 1.

Simulations of MEOSS image analysis were run as single strip adjustments for a striplength of 6 baselength over a periodic terrain model, varying only in the along track direction. Baselength B of MEOSS is 203 km and swath width is 256 km. The adopted terrain model is a saw-tooth shape model which goes up from 0 m to 3000 m in constant slope inclination in 40 km distance and goes down to 0 m with the same slope and this shape is repeated. This terrain is referred as "Mtn." (mountainous) in Table 2. Completely flat terrain model was also tested in simulation runs.

We always used a regular grid of 62 by 7 homologous points on ground, that is roughly 10 meshes per baselengh in along track direction. This meshwidth is somewhat coarse to follow the nutation movement for roll and yaw as can be seen in fig. 1. We never tried less than 7 HP's per scanline, but perhaps 3 might turn out to be sufficient. Fixed weights for each observation are listed in Table 1.

We selected second order for the Gauß processes, corresponding to constant forces in satellite dynamics. We did not try different Gauß-processes.

3.2 Varied Input Parameters

The first simulations with SAEROS run by J.Wu used practically zero weight for the Gauß-processes. Hence convergence had to be forced by additional ground control points and high weights for the initial values. This is the main reason for differences of our results and that given in (5). We calculated the standard weight for the Gauß process individually for every orientation parameter from the expected maximal curvatures. We tried three different weightings for the gauß process by multiplying the unit weights with factors 0.1, 1 and 10.

We used three different levels of noise in image point coordinates 0, 5 and 10 μm (1 σ level) corresponding to 0, 0.5 and 1 pixel. However, we applied always the same weights for the collinearity condition corresponding to 1 σ deviation of 10 μm in the central image strip and 14 μm in the outer ones.

We varied also the number and distribution of ground control points (GCP's). Total number of GCP's in the strip was between 3 and 20.

In other simulation runs done before with four baselength, we tried three ratios of intervals between adjacent orientation stations and along track distances of homologous points. The ratios were 0.5, 1 and 2.

3.3 Simulation Results

Systematic studies need a quite large number of simulation runs. From the comparatively small number of simulations specified above we got the results given in Table 2. The instantaneous field of view IFOV in MEOSS mission is $(0.01\ ^\circ)^2$. This corresponds to 10.7 μm pixel size on focal plane and 73.3 m on ground. These values should be kept in mind for evaluating the results. The preliminary conclusions are:

- Gauß process of second order effectively leads to rapid convergence of the iterative adjustment. We never needed more than four iterations with 1 m convergence criterion for ground coordinates.
- weighting of the Gauß processes seems to be uncritical. Results are rather similar in spite of relative weight factors 0.1, 1 and 10.
- noise in image space positions is a critical factor as shown by fig. 2 to fig. 9.
- when there is no error in image coordinate, very small number of GCP's leads to acceptable results as shown in a test case with only 3 GCP's. However, when there is random errors in image coordinates as in actual case, to increase the number of GCP's improves the results.
- phase distribution of GCP's with regard to baselenth B or nutation period seems to be uncritical. We tried two runs where we set all GCP's to the same phase with regard to baselength B and could not detect important changes. (Run number 6 and 7 in Table

2.) This can also be seen from the fact that simulation with only 3 GCP's reproduced the nutation profile of roll and yaw.

- ratio of orientation interval to distances of adjacent homologous points (along track) should be at least unity or larger. From the results of earlier simulations not shown in Table 2 it followed that a ratio of one half leads to a dependency of the adjusted result on the initial approximations for linearization.

- Terrain shape has practically no influence on accuracy. This can be explained with the low ratio of terrain to satellite heights.

4. Conclusions

From the simulations we conclude that the application of Gauß processes of second order as pseudo observations of orientation parameters is an effective tool to stabilize strip adjustment by homologous points for spaceborne missions of three fold stereoscopic linescan cameras. Therefore other solutions of the geometry problem, like different tilt angles of the CCD scanlines in the focal plane - as recommended in (3) - can be avoided.

5. References

(1) **Lanzl,F.** :"The Three-Line Stereo Camera MEOSS and its Application in Space".- ISPRS Congress in Kyoto, 1988, this volume.

(2) **Ebner,H. and Mueller,F.** :"Processing of Digital Three Line Imagary Using a Generalized Model of Combined Point Determination".- ISPRS Comm.III Symposium in Rovaniemi, Finnland, 11 pages, 1986.

(3) **Hofmann,O.** :"Dynamische Photogrammetrie".- (in German), BuL, Bildmessung und Luftbildwesen, 3/86, pp. 105-121, 1986.

(4) **Drescher,A., Lehner,M. and Wu,J.** :"A Common Approach to Navigation and Geometric Image Correction for the Stereoscopic Linescan Camera MEOSS".- ISPRS Comm.I, Symposium at Stuttgart, FRG, pp.279-284, ESA SP-252), 1986.

(5) **Wu,J.**:"Investigation of Simulated MEOSS-Imagery for Sensor Navigation and Terrain Derivation".- ISPRS Comm.I, Symposium at Stuttgart, FRG, pp.279-284, ESA SP-252, 1986.

TABLE 1. Fixed Weights in the Simulation Runs
(Values are given as a priori standard deviations. Weights are inversely proportional to the squares of these values.)

Ground Control Points		25 m
Image coordinates, Nadir looking		0.01 mm
" , Forward & Backward looking		0.014 mm
Gaussian process, (referred as 'Normal' in TABLE 2.)	XO	0.04 m
	YO	0.01 m
	ZO	0.04 m
	ω	1.29×10^{-3}rad
	ϕ	5.14×10^{-5}rad
	κ	1.29×10^{-3}rad

TABLE 2. Results of Simulation Runs

Run #	INPUT PARAMETERS				RESULTS									
	Number of GCPs	Random Error (1σ)	Weights for Gaussian Process	Terrain Shape	RMSE at check points (meters)				RMSE at orientation stations (m and $\times10^{-5}$rad)					
					X	Y	Z	X,Y,Z	XO	YO	ZO	ω	ϕ	κ
1	9	0	Normal	Mtn.	36.4	76.8	44.3	55.3	45.2	29.0	25.3	19	12	22
2	9	10	Normal	Mtn.	181.4	227.7	338.9	257.9	113.9	939.1	60.7	205	54	78
3					151.5	158.5	357.6	242.2	86.0	653.0	146.2	178	52	81
4					140.7	125.0	341.7	225.2	222.7	855.4	150.5	204	46	63
5					156.8	164.0	303.8	218.9	221.4	553.7	178.6	141	102	61
6	8	0	Normal	Mtn.	61.9	82.1	74.6	73.3	45.1	133.9	74.4	31	15	23
7	8	10	Normal	Mtn.	254.7	178.1	333.7	263.3	110.0	317.2	181.4	90	68	72
8	20	0	Normal	Mtn.	22.4	39.4	36.6	33.6	4.7	15.9	6.0	12	7	27
9	20	5	Normal	Mtn.	64.1	58.8	140.6	95.4	42.1	60.8	22.3	24	27	43
10					56.6	70.7	153.5	102.9	29.7	273.5	11.3	67	20	45
11					41.2	59.1	108.2	75.1	11.5	57.9	4.0	27	19	31
12	20	10	Normal	Mtn.	102.7	152.0	222.9	166.7	62.5	191.1	46.7	48	32	71
13					98.2	125.1	240.1	166.3	22.2	374.7	31.2	96	33	61
14					90.9	101.1	222.9	150.7	100.2	318.6	82.8	74	43	76
15	20	10	×10	Mtn.	90.9	112.5	204.6	144.7	63.2	193.2	28.4	48	34	69
16					122.8	173.3	249.6	189.2	55.0	267.6	82.9	74	46	86
17					94.9	107.5	241.1	162.0	14.3	379.4	41.4	97	49	67
18	20	10	×0.1	Mtn.	103.8	134.9	273.2	185.8	31.1	294.7	33.8	78	50	67
19					80.7	89.6	233.3	151.6	122.8	281.1	48.6	71	38	82
20					90.2	130.9	241.7	167.0	44.4	182.6	66.0	51	45	68
21	20	0	Normal	Flat	24.3	38.4	41.4	35.5	2.6	11.2	9.4	12	8	26
22	20	10	Normal	Flat	107.1	128.2	260.2	178.5	94.3	190.0	18.3	60	44	67
23	3	0	Normal	Mtn.	74.7	51.9	109.3	82.1	21.4	271.8	30.8	67	18	32
24	3	10	Normal	Mtn.	196.9	473.7	500.2	413.7	163.1	722.6	279.4	156	80	143

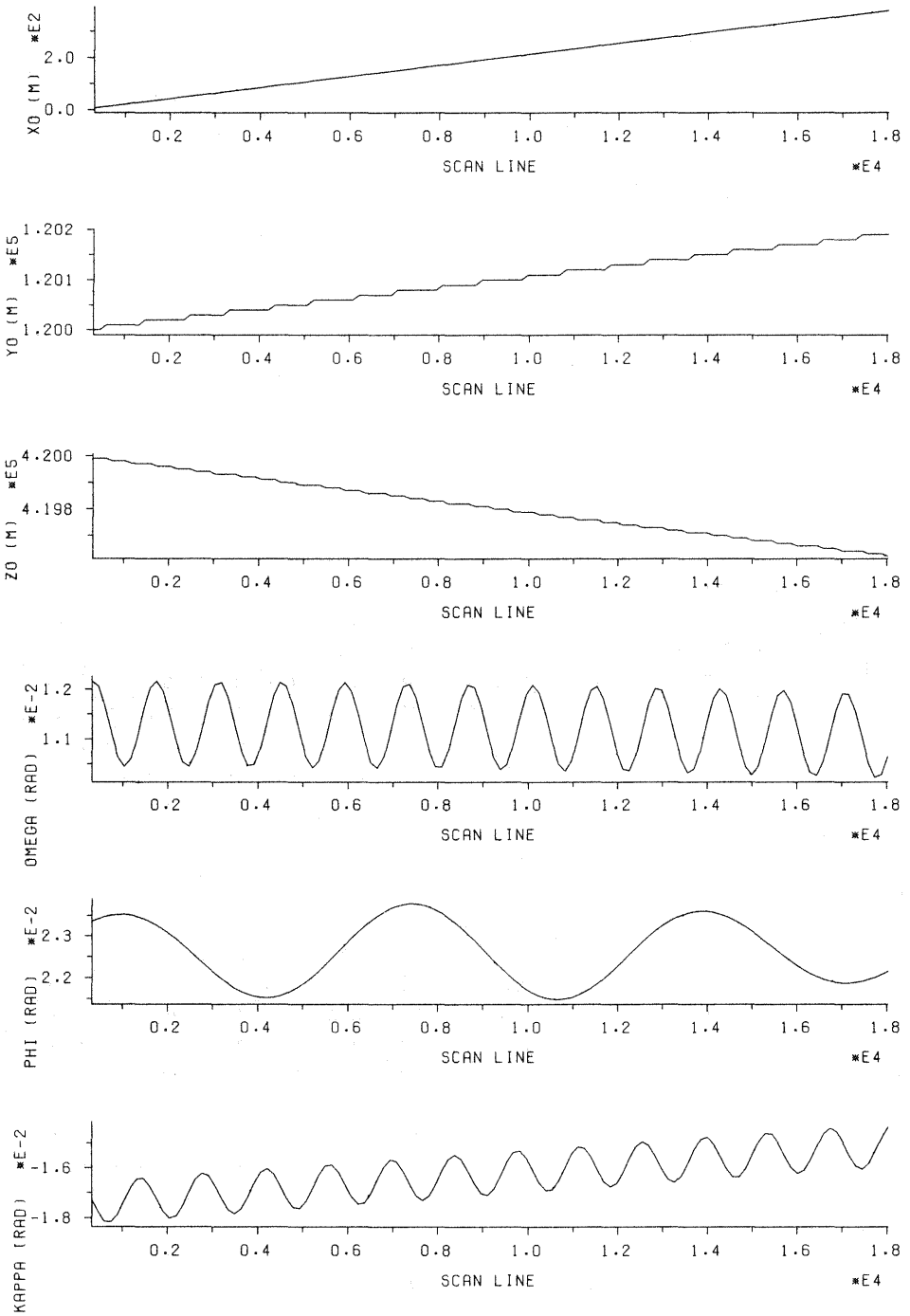

Figure 1. Variation of orientation parameters used as model input

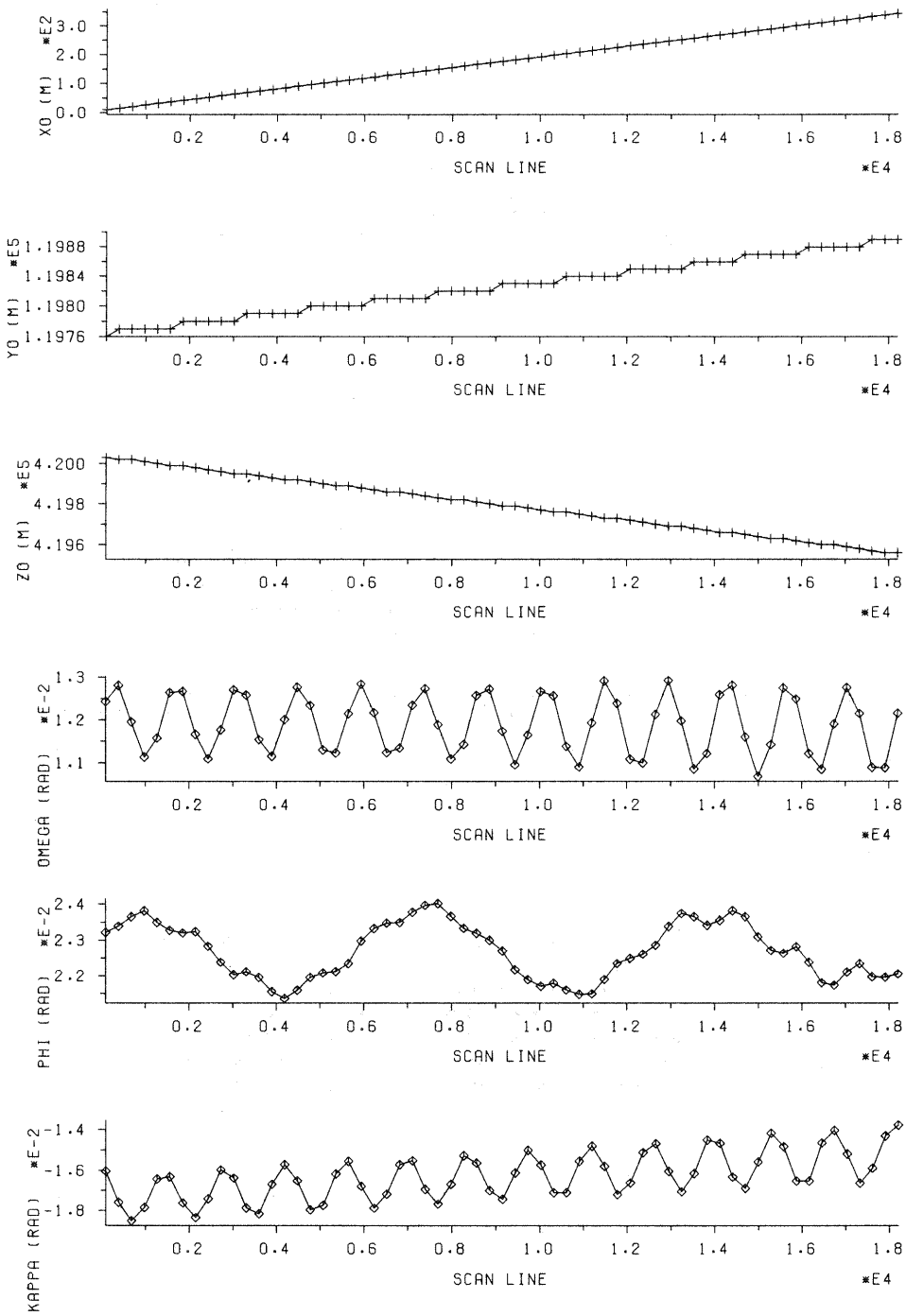

Figure 2. Adjusted orientation parameters (3 GCP's, no image noise, run No.23)

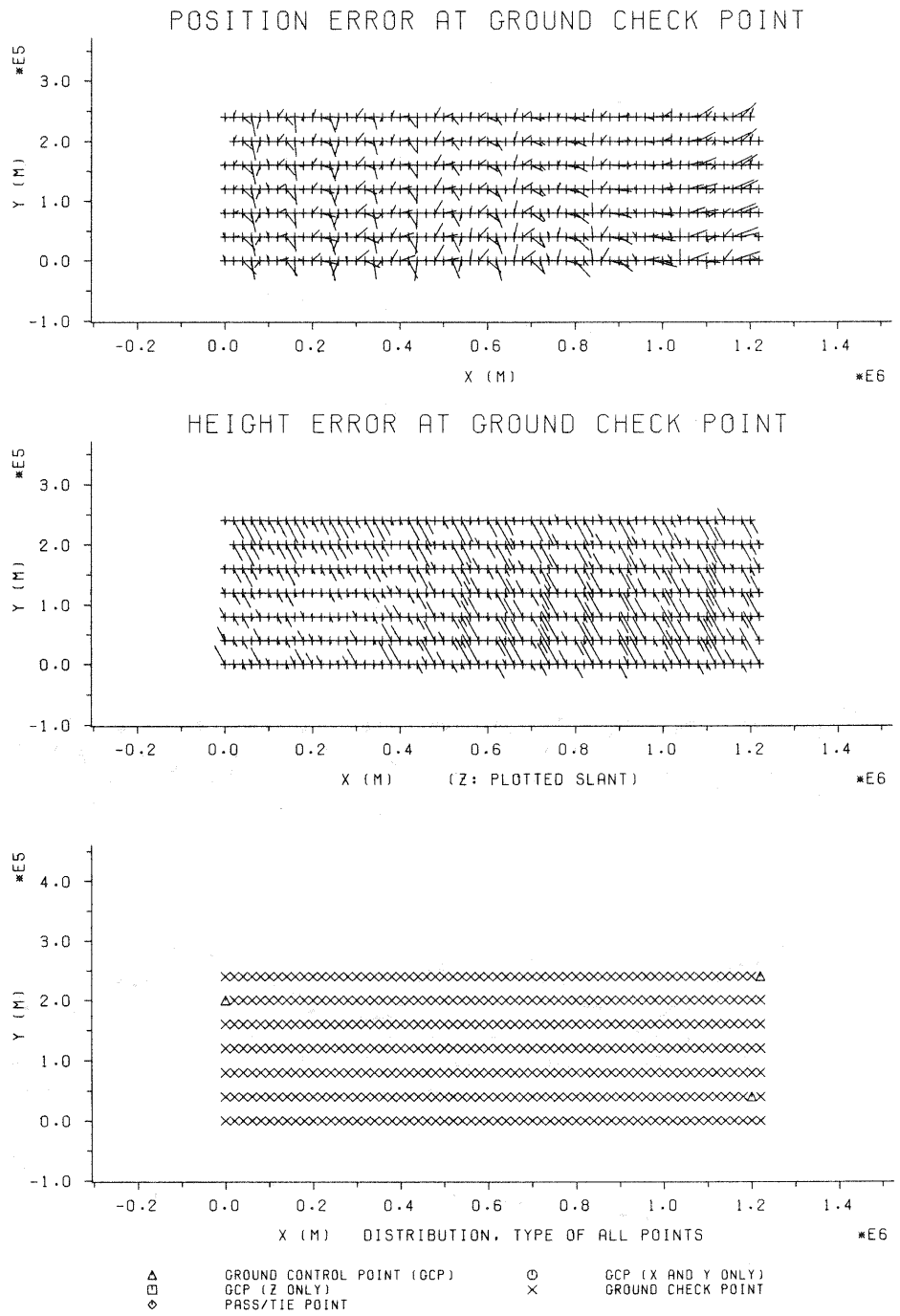

Figure 3. Corresponding errors at ground check points (Error vectors enlarged by factor 270)

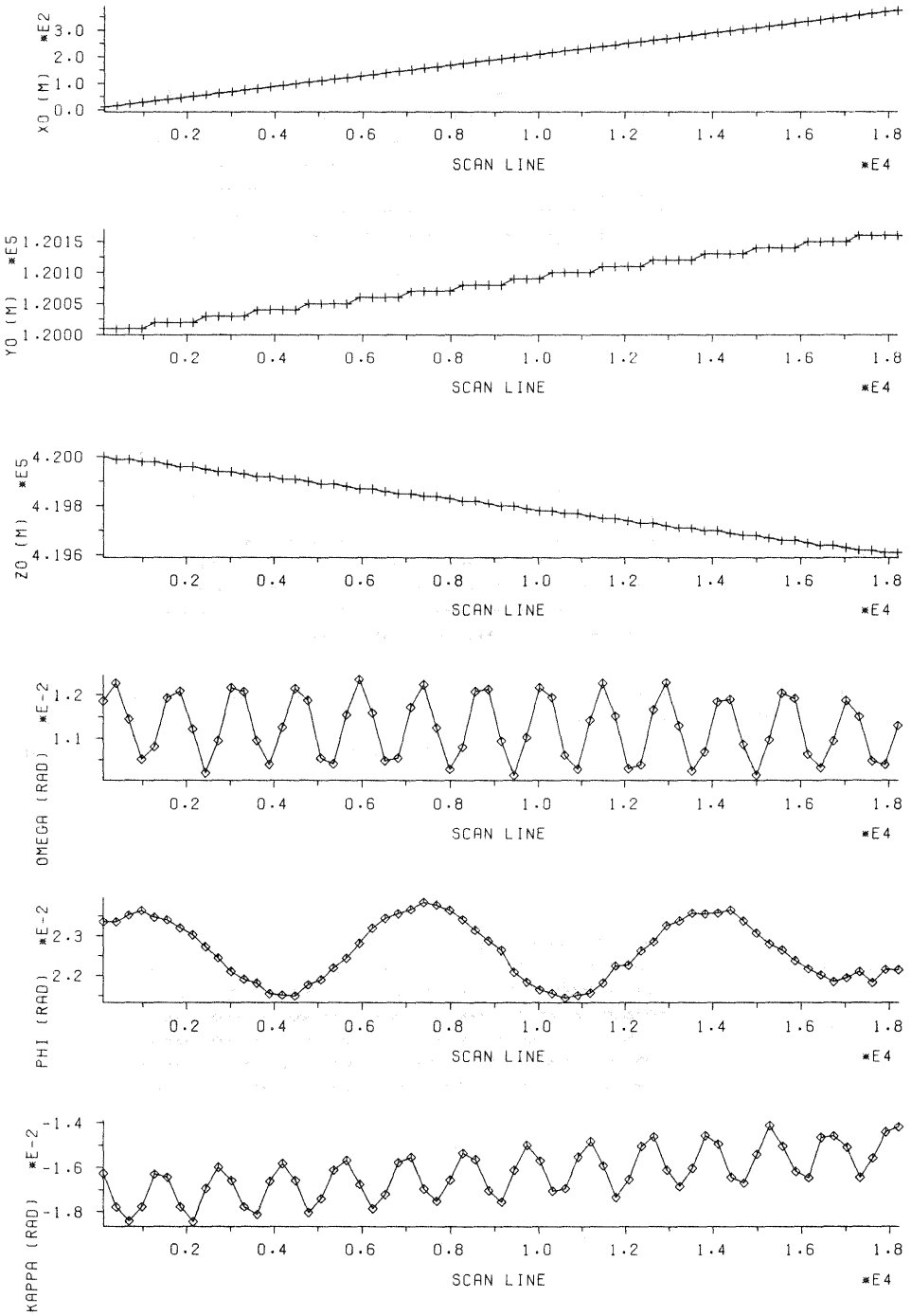

Figure 4. Adjusted orientation parameters (20 GCP's, no image noise, run No.8)

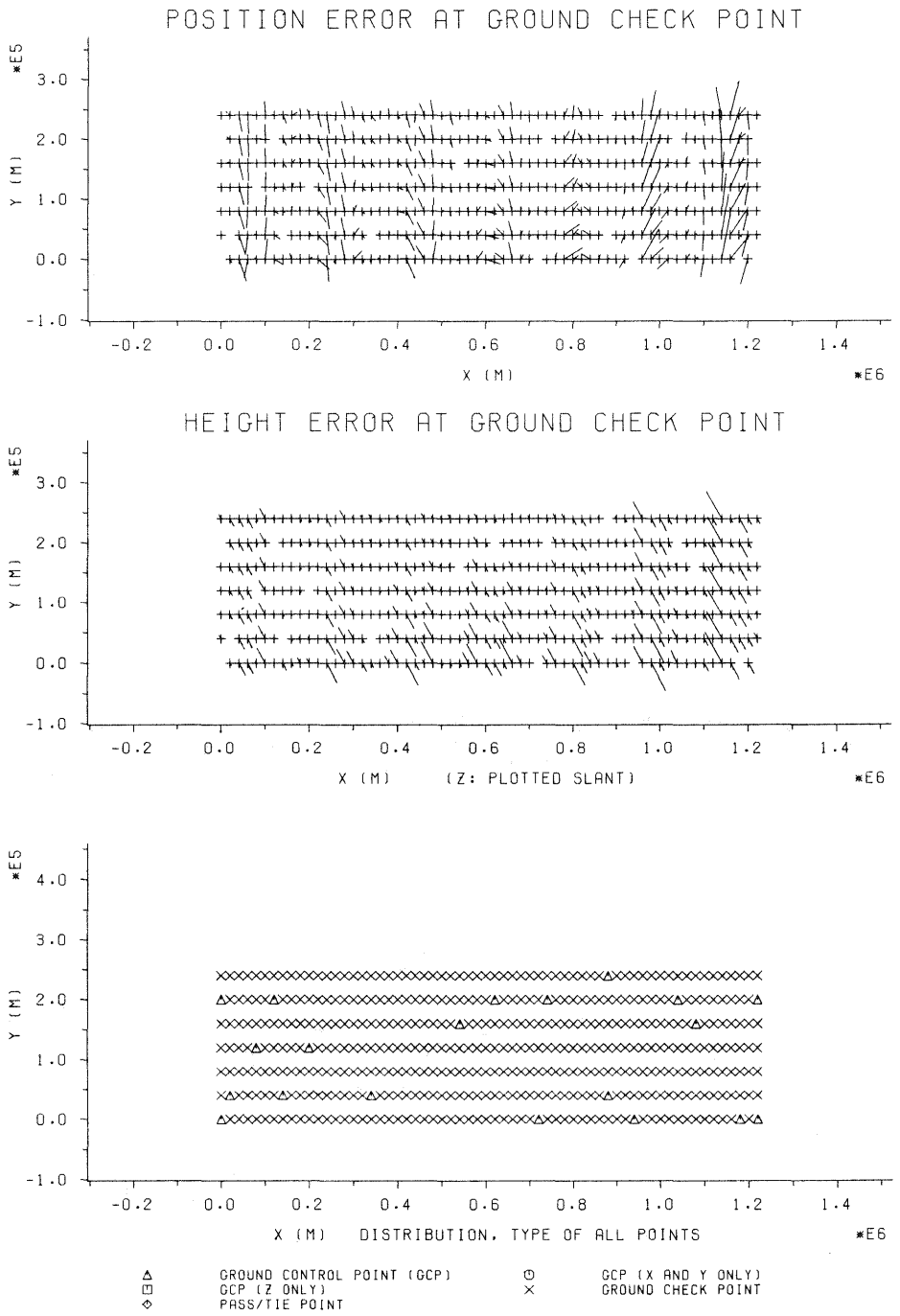

Figure 5. Corresponding errors at ground check points (Error vectors enlarged by factor 460)

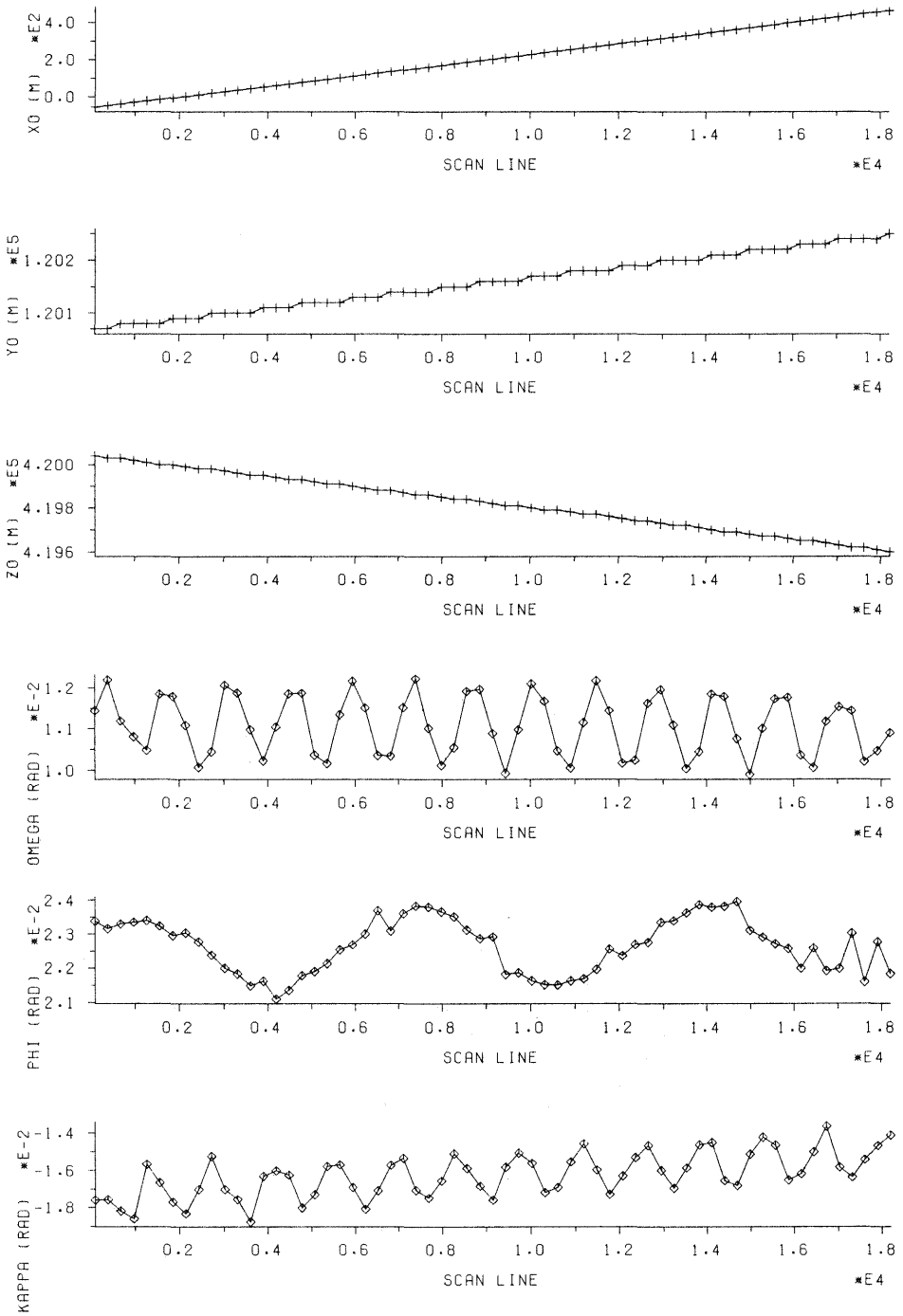

Figure 6. Adjusted orientation parameters (20 GCP's, 5 μm image noise, run No.9)

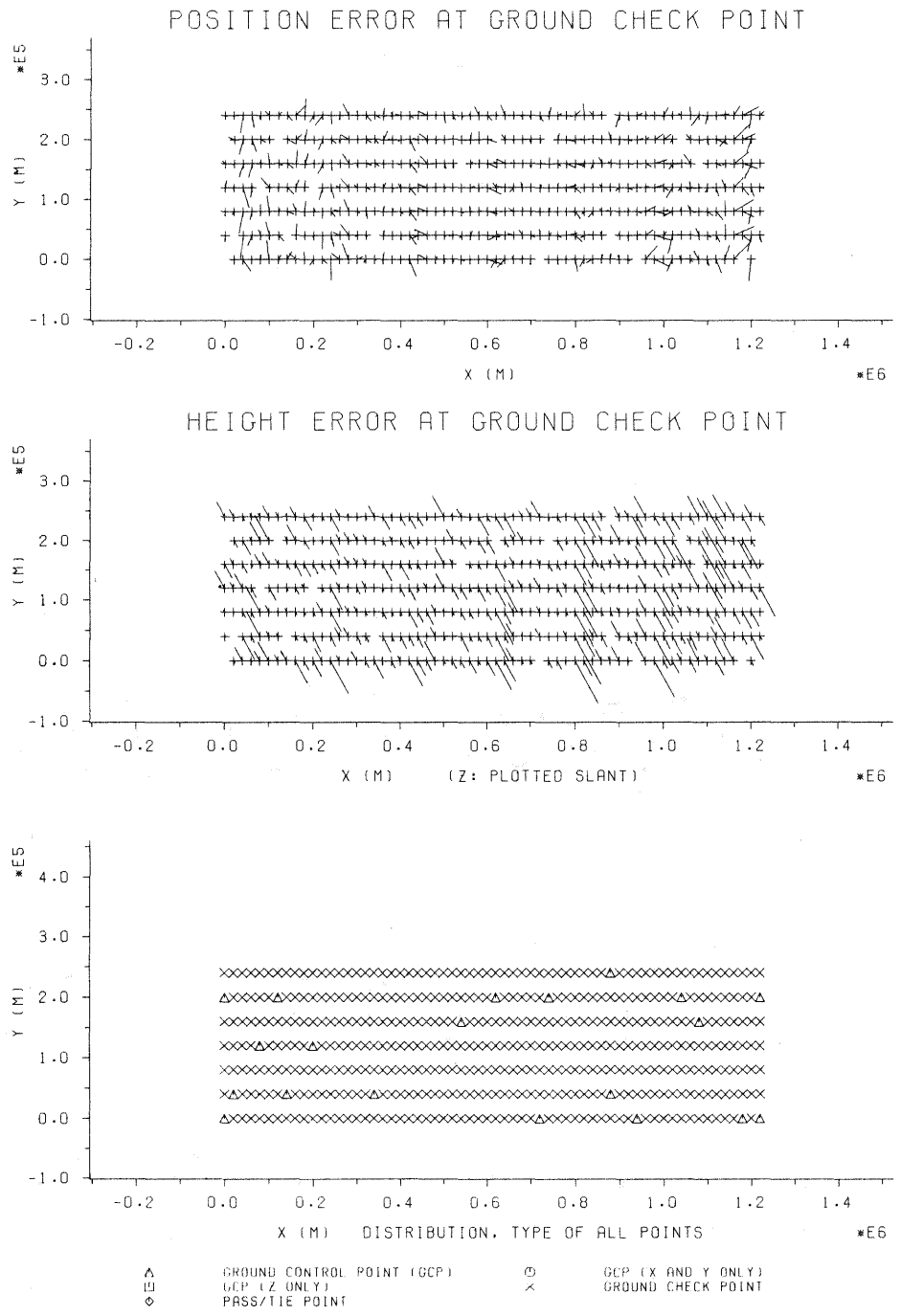

Figure 7. Corresponding errors at ground check points (Error vectors enlarged by factor 190)

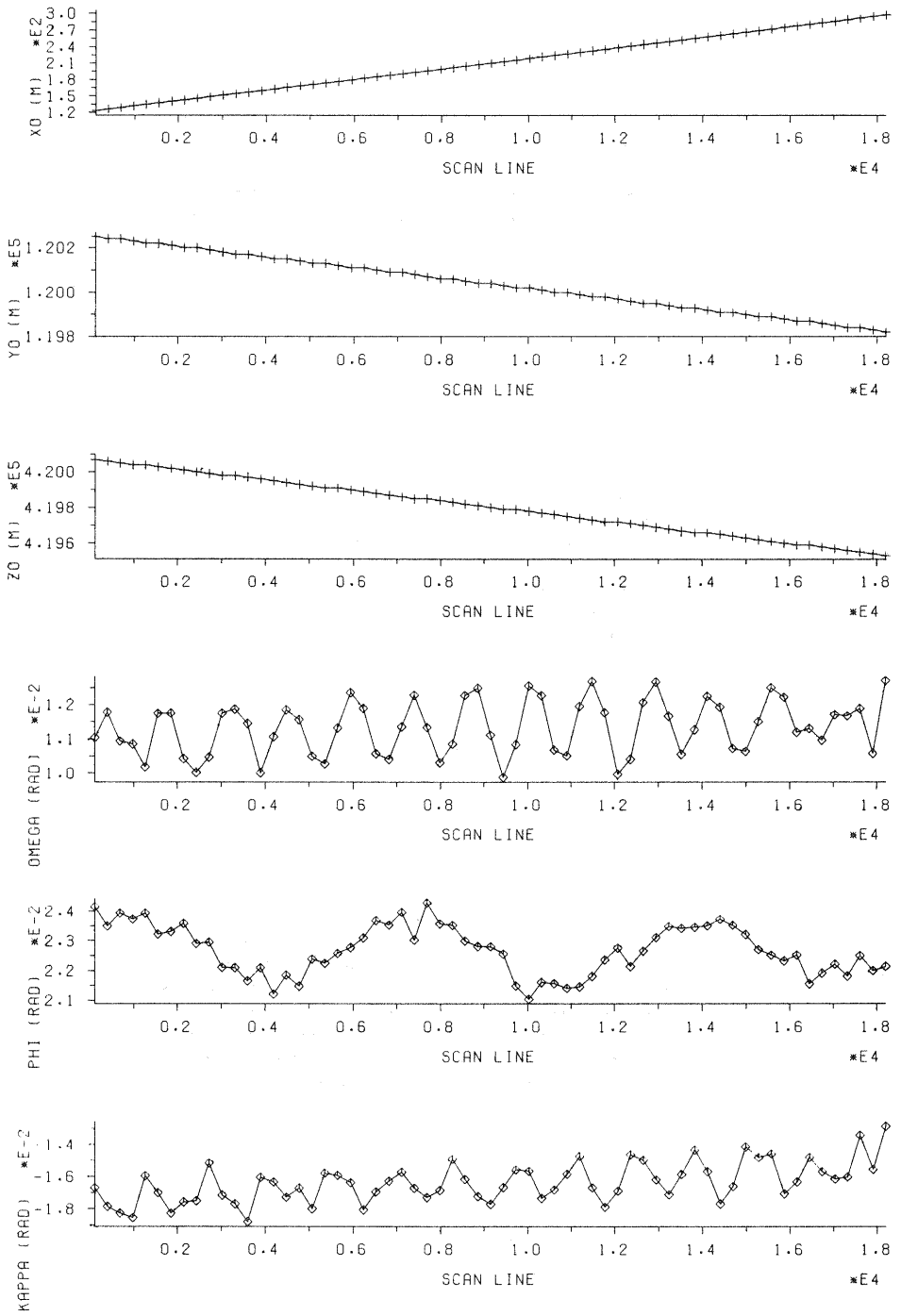

Figure 8. Adjusted orientation parameters (20 GCP's, 10 μm image noise, run No.12)

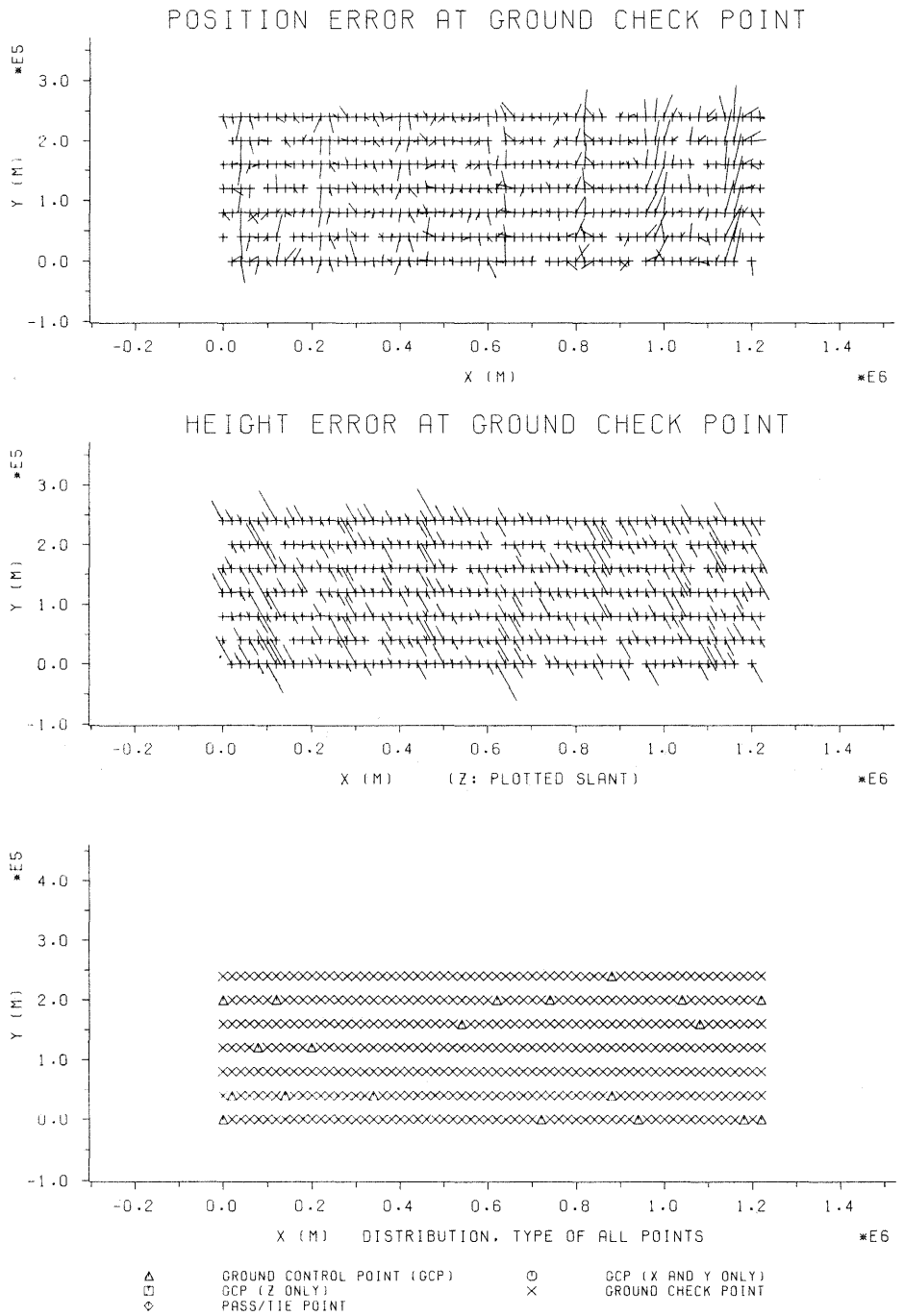

Figure 9. Corresponding errors at ground check points (Error vectors enlarged by factor 120)